

# Generating correlated (2+1)-photon in an active Raman gain medium

Cui-Ping Lu, Chun-Hua Yuan, and Weiping Zhang  
State Key Laboratory of Precision Spectroscopy, Department of Physics,  
East China Normal University, Shanghai 200062, P. R. China

L. Deng

Electron and Optical Physics Division, National Institute of Standards & Technology, Gaithersburg, Maryland 20899, USA

(Dated: October 27, 2018)

A scheme of generating controllable (2+1) photons in a double- $\Lambda$  atomic system based on active-Raman-gain is presented in this paper. Such (2+1) photons can be a potential candidate to generate a correlated photon pair as the photon '1' acts as a trigger. Compared to other schemes of generating correlated photon pairs, our scheme exhibits a number of advantages due to the exploit of the stimulated Raman process.

PACS numbers: 42.65.Dr, 42.50.Dv, 42.25.Bs

## I. INTRODUCTION

Spontaneous parametric down-conversion (SPDC) is a widely used method for producing correlated and entangled photon pairs. Due to the spontaneous emission nature of the process, SPDC-based single-photon sources usually have limited applications because of broadband spectrum, low efficiency, short coherence time and coherence length. Recently, electromagnetically induced transparency (EIT) technique has been used by two groups to generate paired photons in an otherwise opaque atomic medium [1, 2]. Balić *et al.* [3] have demonstrated the generation of counter-propagating paired photons in a double- $\Lambda$  four wave mixing (FWM) scheme where the anti-Stokes/FWM field is generated under the EIT condition. With a modified scheme Kolchin *et al.* [4] have shown the generation of narrowband photon pairs using a standing wave produced by a single intense driving laser. Thompson *et al.* [5] have reported the generation of narrowband pairs of photons from a laser-cooled atomic ensemble inside an optical cavity. Du *et al.* [6] have reported the production of biphotons in a two-level atomic system. A key element of these experiments is that one photon is generated by the spontaneous Raman emission process whereas the second photon is generated via an EIT-assisted two-wave mixing process. Alternatively, the process can be viewed as a FWM generation with one spontaneous emission step in the wave mixing loop.

In this paper, we present a far-detuned, active Raman gain (ARG) scheme [7, 8, 9, 10] for the generation of a group of correlated (2+1) photons. At the first glance the scheme reported here is very similar to those studied in Ref.[1, 2, 3, 4, 5, 6]. However, it is operated under a very different principle. Instead of relying on a spontaneous Raman process to generate the first photon, we inject a probe photon which leads to stimulated Raman generation. Two improvements are immediately clear: (1) injection-seeding of the probe photon leads to highly directional generation of probe photons and FWM photons, and (2) stimulated Raman process ensures that the more

photons appear in the same frequency mode and the gain can be easily controllable. The first improvement significantly increases detection efficiency in comparison with a process that relies on spontaneous emission of the first photon. Due to stimulated emission the generated probe field has the band width and frequency characteristics exactly as the inject-seeding field. The second improvement eliminates the deficiency usually associated with a typical SPDC-based photon pairs generation technique where a group of *two photons* are generated simultaneously. The reason is as follows. For a subsequent experiment, one of the photon constituting the pair is often needed as a trigger or coincidence indicator, leaving only one photon for the subsequent experiment in the SPDC-based case. Consequently, one is often not able to study correlation properties of the pair as they propagate through a second working medium. By choosing the gain of the active Raman process, we can achieve a special mode of operation where only one photon is stimulated-generated by the injected single probe photon. Carefully choosing the detuning and intensity of the second pump field, we can generate a group of (2+1) photons where two photons are in the same probe frequency mode whereas one photon in the FWM frequency mode. With this pair/group generation technique one of probe photons can now be used as a coincidence indicator but we still have a pair of correlated photons (one in probe mode and one in FWM mode) for the subsequent correlated-photon-pair propagation experiment. This arrangement clearly has advantages and may be applied to various photon-pair experiments where a correlated pair plus a correlated trigger photon are required.

We consider an ensemble of identical lifetime broadened four-state atoms initially prepared in their ground states  $|1\rangle$  by suitable optical pumping method. The schematic of the process considered here is shown in Fig. 1. A strong cw pump field ( $E_{P1}$ ) couples the ground state  $|1\rangle$  to an excited state  $|2\rangle$  with a large one-photon detuning  $\delta_1$ . A second cw laser field ( $E_{P2}$ ) couples the state  $|3\rangle$  to an excited state  $|4\rangle$  with the detuning  $\Delta + \delta_4$ . A single probe photon field  $\hat{E}_1$  (with central frequency

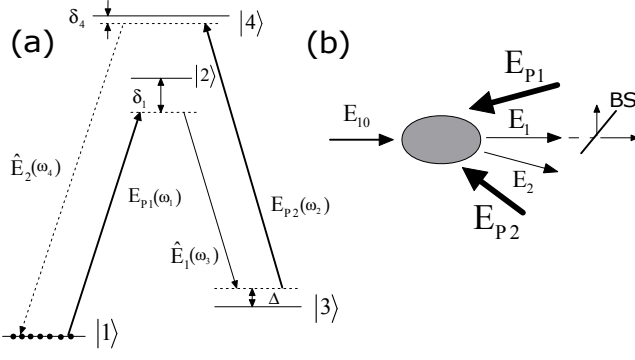


FIG. 1: (Color online) (a) Schematic atomic level diagram.  $E_{P1}(\omega_1)$  and  $E_{P2}(\omega_2)$  are the pump fields, and  $\hat{E}_1(\omega_3)$  is the probe field.  $\hat{E}_2(\omega_4)$  describes the process of another photon ( $\omega_4$ ) generated by FWM. (b) Schematic of the experiment for 2+1 photons generation.

$\omega_3$ ), which couples the state  $|2\rangle$  to a lower excited state  $|3\rangle$ , is then introduced to the medium. Consequently, a two-photon Raman transition can occur, causing an atom to absorb a pump photon and emit a photon into the probe field frequency mode. The presence of the second pump field subsequently pumps the atom to state  $|4\rangle$  and a FWM process occurs, leading to the generation of a new photon at the frequency  $\omega_4 = \omega_1 - \omega_3 + \omega_2$ . In such a process two photons at  $\omega_3$  as well as one photon at  $\omega_4$  are simultaneously generated, yielding a group of (2+1) correlated photons [11].

The paper is organized as follows. In Sec. II we first derive the equations of motion for atomic dynamics and field propagation equations. With analytical solutions we first examine a limiting case where our scheme reduces to a well-known single  $\Lambda$  gain scheme. We then investigate group velocities of various propagation modes and corresponding propagation parameters for the injection-seeded double- $\Lambda$  scheme. In Sec. III, we consider the case where a single-photon wave-packet quantum probe field is injected into the medium and we investigate the generation and propagation of the two probe photons and one FWM photon under the condition of weak gain. We also analyze the atomic state vector and photon cross correlation function. In Sec. IV, we discuss possible complications due to various ac Stark effects. We also discuss the case where the input probe field is a coherent state and obtain the single-photon-added coherent state. A summary is given in Sec. V.

## II. MODEL AND ANALYSIS

### A. Theoretical Model

In the electric-dipole and rotating-wave approximations, the interaction Hamiltonian of  $N$  identical four-state atoms interacting with laser fields (see Fig. 1) is

given as ( $\hbar = 1$ )

$$\begin{aligned} \hat{H}_I^j = & -(\Omega_1 e^{i\vec{k}_1 \cdot \vec{r}_j - i\omega_1 t} \hat{\sigma}_{21}^j + \Omega_2 e^{i\vec{k}_2 \cdot \vec{r}_j - i\omega_2 t} \hat{\sigma}_{43}^j \\ & + g_1 \hat{E}_1^{(+)} e^{i\vec{k}_3 \cdot \vec{r}_j - i\omega_3 t} \hat{\sigma}_{23}^j + g_2 \hat{E}_2^{(+)} e^{i\vec{k}_4 \cdot \vec{r}_j - i\omega_4 t} \hat{\sigma}_{41}^j + \text{H.c.}), \end{aligned} \quad (1)$$

where  $\hat{E}_q^{(+)}(z, t)$  is the positive frequency component of the quantum field operator ( $q = 1, 2$  are for probe and FWM field, respectively),  $\hat{E}_q^{(-)} = (\hat{E}_q^{(+)})^\dagger$ , and  $\hat{\sigma}_{kl}^j = |k\rangle_{jj}\langle l|$  ( $k, l = 1, 2, 3, 4$ ). In addition,  $2\Omega_1 = \mu_{21} E_{P1}/\hbar$  and  $2\Omega_2 = \mu_{43} E_{P2}/\hbar$  are Rabi frequencies of pump fields with  $\mu_{nn'}$  being the dipole matrix element for the  $|n\rangle - |n'\rangle$  transition and  $E_{P1, P2}$  being the amplitudes of the two classical pump fields.  $g_1$  and  $g_2$  are the atom-photon coupling constants, and  $\omega_m$  and  $\vec{k}_m$  ( $m = 1, 2, 3, 4$ ) are the carrier frequency and wave vector of the  $m$ -th optical field, respectively.

We define continuum atomic operators  $\hat{\sigma}_{\mu\nu}$  by summing over the individual atoms in a small volume  $V$ , and introduce slowly varying atomic operators  $\tilde{\sigma}_{\mu\nu}$ :  $\sigma_{12} = e^{-i\omega_1 t} \tilde{\sigma}_{12}$ ,  $\sigma_{13} = e^{i(\omega_3 - \omega_1)t} \tilde{\sigma}_{13} = e^{i(\omega_2 - \omega_4)t} \tilde{\sigma}_{13}$ ,  $\sigma_{14} = e^{-i\omega_4 t} \tilde{\sigma}_{14}$ ,  $\sigma_{23} = e^{i\omega_3 t} \tilde{\sigma}_{23}$ ,  $\sigma_{24} = e^{-i(\omega_4 - \omega_1)t} \tilde{\sigma}_{24} = e^{-i(\omega_2 - \omega_3)t} \tilde{\sigma}_{24}$ ,  $\sigma_{34} = e^{-i\omega_2 t} \tilde{\sigma}_{34}$ , the equations for the atomic operators in the Heisenberg picture are

$$\begin{aligned} \dot{\tilde{\sigma}}_{21} = & -(\gamma_{21} - i\delta_1) \tilde{\sigma}_{21} + i\Omega_1^* e^{-i\vec{k}_1 \cdot \vec{r}} (\sigma_{22} - \sigma_{11}) \\ & + ig_2 \hat{E}_2^{(-)} e^{-i\vec{k}_4 \cdot \vec{r}} \tilde{\sigma}_{24} - ig_1 \hat{E}_1^{(-)} e^{-i\vec{k}_3 \cdot \vec{r}} \tilde{\sigma}_{31}, \end{aligned} \quad (2a)$$

$$\begin{aligned} \dot{\tilde{\sigma}}_{34} = & -(\gamma_{34} + i\delta_2) \tilde{\sigma}_{34} - i\Omega_2 e^{i\vec{k}_2 \cdot \vec{r}} (\sigma_{44} - \sigma_{33}) \\ & - ig_1 \hat{E}_1^{(+)} e^{i\vec{k}_3 \cdot \vec{r}} \tilde{\sigma}_{24} + ig_2 \hat{E}_2^{(+)} e^{i\vec{k}_4 \cdot \vec{r}} \tilde{\sigma}_{31}, \end{aligned} \quad (2b)$$

$$\begin{aligned} \dot{\tilde{\sigma}}_{31} = & -(\gamma_{31} - i\Delta) \tilde{\sigma}_{31} + i\Omega_1^* e^{-i\vec{k}_1 \cdot \vec{r}} \tilde{\sigma}_{32} - i\Omega_2 e^{i\vec{k}_2 \cdot \vec{r}} \tilde{\sigma}_{41} \\ & - ig_1 \hat{E}_1^{(+)} \tilde{\sigma}_{21} e^{i\vec{k}_3 \cdot \vec{r}} + ig_2 \hat{E}_2^{(-)} e^{-i\vec{k}_4 \cdot \vec{r}} \tilde{\sigma}_{34}, \end{aligned} \quad (2c)$$

$$\begin{aligned} \dot{\tilde{\sigma}}_{41} = & -(\gamma_{41} - i\delta_4) \tilde{\sigma}_{41} + i\Omega_1^* e^{-i\vec{k}_1 \cdot \vec{r}} \tilde{\sigma}_{42} - i\Omega_2^* e^{-i\vec{k}_2 \cdot \vec{r}} \tilde{\sigma}_{31} \\ & - ig_2 \hat{E}_2^{(-)} (\sigma_{11} - \sigma_{44}) e^{-i\vec{k}_4 \cdot \vec{r}}, \end{aligned} \quad (2d)$$

$$\begin{aligned} \dot{\tilde{\sigma}}_{32} = & -(\gamma_{32} + i\delta_3) \tilde{\sigma}_{32} + i\Omega_1 e^{i\vec{k}_1 \cdot \vec{r}} \tilde{\sigma}_{31} - i\Omega_2 e^{i\vec{k}_2 \cdot \vec{r}} \tilde{\sigma}_{42} \\ & - ig_1 \hat{E}_1^{(+)} (\sigma_{22} - \sigma_{33}) e^{i\vec{k}_3 \cdot \vec{r}}, \end{aligned} \quad (2e)$$

$$\begin{aligned} \dot{\tilde{\sigma}}_{42} = & -[\gamma_{42} - i(\delta_1 - \delta_4)] \tilde{\sigma}_{42} + i\Omega_1 \tilde{\sigma}_{41} e^{i\vec{k}_1 \cdot \vec{r}} - i\Omega_2^* \tilde{\sigma}_{32} \\ & \times e^{-i\vec{k}_2 \cdot \vec{r}} + ig_1 \hat{E}_1^{(+)} \tilde{\sigma}_{43} e^{i\vec{k}_3 \cdot \vec{r}} \\ & - ig_2 \hat{E}_2^{(-)} \tilde{\sigma}_{12} e^{-i\vec{k}_4 \cdot \vec{r}}, \end{aligned} \quad (2f)$$

where  $\delta_1 = \omega_{21} - \omega_1$ ,  $\delta_2 = \omega_{43} - \omega_2$ ,  $\delta_3 = \omega_{23} - \omega_3$ ,  $\delta_4 = \omega_{41} - \omega_4$ ,  $\Delta = \delta_3 - \delta_1 = \delta_2 - \delta_4$ , and  $\omega_{kl} = \omega_k - \omega_l$  is the frequency of the  $|k\rangle \leftrightarrow |l\rangle$  transition.  $\gamma_{kl}$  ( $\gamma_{kl} = \gamma_{lk}$ ) is the dephasing rate between state  $|k\rangle$  and state  $|l\rangle$ .

Using the slowly varying envelope and unfocused plane wave approximations, we obtain the following propagation equations for the quantum field operators:

$$\left[ \left( c \frac{\partial}{\partial z} + \frac{\partial}{\partial t} \right) \hat{E}_1^{(+)}(z, t) \right] e^{i\vec{k}_3 \cdot \vec{r}} = ig_1 N \tilde{\sigma}_{32}, \quad (3)$$

$$\left[ \left( c \frac{\partial}{\partial z} + \frac{\partial}{\partial t} \right) \hat{E}_2^{(-)}(z, t) \right] e^{-i\vec{k}_4 \cdot \vec{r}} = -ig_2 N \tilde{\sigma}_{41}. \quad (4)$$

Under the condition that the probe field is much weaker than the pump fields, and using the assumption that pump fields propagate without depletion, Eq. (2a) and Eq. (2f) can be evaluated adiabatically

$$\tilde{\sigma}_{21}^{(0)} \approx \frac{\Omega_1^* e^{-i\vec{k}_1 \cdot \vec{r}}}{\delta_1 + i\gamma_{21}}, \quad \tilde{\sigma}_{42}^{(0)} \approx \frac{\Omega_1 \tilde{\sigma}_{41} e^{i\vec{k}_1 \cdot \vec{r}} - \Omega_2^* \tilde{\sigma}_{32} e^{-i\vec{k}_2 \cdot \vec{r}}}{\delta_4 - \delta_1 - i\gamma_{42}}. \quad (5)$$

Considering  $\sigma_{22}^{(0)} = \sigma_{33}^{(0)} = \sigma_{44}^{(0)} = \tilde{\sigma}_{34}^{(0)} \approx 0$ , and substituting these values of the density matrix elements into Eqs. (2c)-(2e), we obtain the following set of coupled equations:

$$\begin{cases} \dot{\tilde{\sigma}}_{31} = -(\gamma_{31} - i\Delta)\tilde{\sigma}_{31} + i\Omega_1^* e^{-i\vec{k}_1 \cdot \vec{r}} \tilde{\sigma}_{32} \\ \quad - i\Omega_2 e^{i\vec{k}_2 \cdot \vec{r}} \tilde{\sigma}_{41} - ig_1 \tilde{\sigma}_{21} \hat{E}_1^{(+)}(z, t) e^{i\vec{k}_3 \cdot \vec{r}}, \\ \dot{\tilde{\sigma}}_{41} = -(\gamma_{41} - i\delta_4)\tilde{\sigma}_{41} + i\Omega_1^* e^{-i\vec{k}_1 \cdot \vec{r}} \tilde{\sigma}_{42} \\ \quad - i\Omega_2^* e^{-i\vec{k}_2 \cdot \vec{r}} \tilde{\sigma}_{31} - ig_2 \hat{E}_2^{(-)}(z, t) e^{-i\vec{k}_4 \cdot \vec{r}}, \\ \dot{\tilde{\sigma}}_{32} = -(\gamma_{32} + i\delta_3)\tilde{\sigma}_{32} + i\Omega_1 \tilde{\sigma}_{31} e^{i\vec{k}_1 \cdot \vec{r}} - i\Omega_2 e^{i\vec{k}_2 \cdot \vec{r}} \tilde{\sigma}_{42}. \end{cases} \quad (6)$$

Substituting Eq. (5) into Eq. (6), we make the Fourier transform and obtain the solutions for  $\tilde{\sigma}_{32}$  and  $\tilde{\sigma}_{41}$  in the frequency domain

$$\Sigma_{32} = -\frac{g_1 |\Omega_1|^2 (\omega - d_4)}{d_1 D(\omega)} \hat{\epsilon}_1(z, \omega) e^{i\vec{k}_3 \cdot \vec{r}} + \frac{g_2 \Omega_1 \Omega_2}{D(\omega)} \hat{\epsilon}_2^\dagger(z, -\omega) e^{i(\vec{k}_1 + \vec{k}_2 - \vec{k}_4) \cdot \vec{z}}, \quad (7)$$

$$\Sigma_{41} = \frac{g_1 \Omega_1^* \Omega_2^* (\omega + d_3)}{d_1 D(\omega)} \hat{\epsilon}_1(z, \omega) e^{-i(\vec{k}_1 + \vec{k}_2 - \vec{k}_3) \cdot \vec{r}} - \frac{g_2 [(\omega - d_2)(\omega + d_3) - |\Omega_1|^2]}{D(\omega)} \hat{\epsilon}_2^\dagger(z, -\omega) e^{-i\vec{k}_4 \cdot \vec{r}}, \quad (8)$$

where  $d_1 = \delta_1 + i\gamma_{21}$ ,  $d_2 = \Delta + i\gamma_{31}$ ,  $d_3 = \delta_3 - i\gamma_{32}$ ,  $d_4 = \delta_4 + i\gamma_{41}$ , and  $D(\omega) = (\omega - d_2)(\omega + d_3)(\omega - d_4) - |\Omega_1|^2(\omega - d_4) - |\Omega_2|^2(\omega + d_3)$ . In addition,  $\hat{\epsilon}_j(z, \omega) = \int_{-\infty}^{\infty} \hat{E}_j^{(+)}(z, t) e^{-i\omega t} dt$ , and  $\Sigma_{32}(z, \omega)$  and  $\Sigma_{41}(z, \omega)$  are Fourier transforms of  $\sigma_{32}(z, t)$  and  $\sigma_{41}(z, t)$ , with  $\omega$  being the transform variable, respectively. Making the Fourier transform of Eqs. (3) and (4) and using Eqs. (7) and (8) we obtain

$$\frac{\partial}{\partial z} \hat{\epsilon}_1(z, \omega) = -\frac{i\omega}{c} \hat{\epsilon}_1(z, \omega) - iD_1(\omega) \hat{\epsilon}_1(z, \omega) - iD_2(\omega) \hat{\epsilon}_2^\dagger(z, -\omega) e^{i\Delta k z}, \quad (9)$$

$$\frac{\partial}{\partial z} \hat{\epsilon}_2^\dagger(z, -\omega) = -\frac{i\omega}{c} \hat{\epsilon}_2^\dagger(z, -\omega) - iD_3(\omega) \hat{\epsilon}_1(z, \omega) e^{-i\Delta k z} - iD_4(\omega) \hat{\epsilon}_2^\dagger(z, -\omega), \quad (10)$$

where

$$\begin{aligned} D_1(\omega) &= \frac{K_1 |\Omega_1|^2 (\omega - d_4)}{d_1 D(\omega)}, \quad D_2(\omega) = -\frac{K_{12} \Omega_1 \Omega_2}{D(\omega)}, \\ D_3(\omega) &= \frac{K_{12} \Omega_1^* \Omega_2^* (\omega + d_3)}{d_1 D(\omega)}, \\ D_4(\omega) &= \frac{K_2 [|\Omega_1|^2 - (\omega - d_2)(\omega + d_3)]}{D(\omega)}, \end{aligned} \quad (11)$$

in which  $K_1 = \frac{N|g_1|^2}{c}$ ,  $K_2 = \frac{N|g_2|^2}{c}$ ,  $K_{12} = \frac{Ng_1 g_2}{c}$ , and phase mismatch  $\Delta k = \vec{k}_4 - \vec{k}_3 + \vec{k}_2 - \vec{k}_1$ . Equations (9) and (10) can be solved analytically for arbitrary initial conditions. For simplicity, we let the phase mismatch  $\Delta k = 0$ . The solutions of Eqs. (9) and (10) are as follows

$$\hat{\epsilon}_1(z, \omega) = \frac{1}{U_+ U_- - 1} [(U_+ U_- e^{-i\lambda_+ z} - e^{-i\lambda_- z}) \hat{\epsilon}_{10}(0, \omega) + U_+ (e^{-i\lambda_- z} - e^{-i\lambda_+ z}) \hat{\epsilon}_{20}^\dagger(0, -\omega)], \quad (12)$$

$$\hat{\epsilon}_2^\dagger(z, -\omega) = \frac{1}{U_+ U_- - 1} [U_- (e^{-i\lambda_+ z} - e^{-i\lambda_- z}) \hat{\epsilon}_{10}(0, \omega) + (U_+ U_- e^{-i\lambda_- z} - e^{-i\lambda_+ z}) \hat{\epsilon}_{20}^\dagger(0, -\omega)], \quad (13)$$

where

$$\begin{aligned} \lambda_\pm &= \frac{\omega}{c} + \frac{1}{2} [D_1(\omega) + D_4(\omega) \mp D_5(\omega)], \\ U_+ &= \frac{2D_2(\omega)}{D_4(\omega) - D_1(\omega) - D_5(\omega)}, \\ U_- &= -\frac{2D_3(\omega)}{D_4(\omega) - D_1(\omega) - D_5(\omega)}, \\ D_5(\omega) &= \sqrt{(D_1(\omega) - D_4(\omega))^2 + 4D_2(\omega)D_3(\omega)}. \end{aligned} \quad (14)$$

We focus our attention on the adiabatic regime [12], where  $\lambda_\pm$  and  $U_\pm$  can be expanded into a rapidly converging power series of dimensionless transform variable  $\zeta = \omega\tau$  where  $\tau$  is the pulse duration of the weak probe field. In this regime [12],  $U_\pm = W_\pm + \mathcal{O}(\zeta)$  and  $\lambda_\pm = (\lambda_\pm)_{\zeta=0} + \zeta/V_{g\pm} + \mathcal{O}(\zeta^2)$  can accurately describe the FWM generation and propagation process. The expansions can be well valid close to the central frequency component of the field. The inverse Fourier transform of Eqs. (12) and (13) are given by

$$\hat{E}_1^{(+)}(z, t) = [A_1 \hat{\epsilon}_{10} - A_2 \hat{\epsilon}_{20}^\dagger] P_{p1}(\eta_+) e^{\beta_+ z} + [A_2 \hat{\epsilon}_{20}^\dagger - A \hat{\epsilon}_{10}] P_{p1}(\eta_-) e^{\beta_- z}, \quad (15)$$

$$\hat{E}_2^{(-)}(z, t) = [A_3 \hat{\epsilon}_{10} - A \hat{\epsilon}_{20}^\dagger] P_{p1}(\eta_+) e^{\beta_+ z} + [A_1 \hat{\epsilon}_{20}^\dagger - A_3 \hat{\epsilon}_{10}] P_{p1}(\eta_-) e^{\beta_- z}, \quad (16)$$

where  $A = 1/(W_+ W_- - 1)$ ,  $A_1 = W_+ W_- A$ ,  $A_2 = W_+ A$ ,  $A_3 = W_- A$ ,  $\eta_\pm = t - z/V_{g\pm}$ ,  $\beta_\pm = -i(\lambda_\pm)_{\zeta=0}$  and  $P_{p1}(t)$  is the pulse shape function for the initial single photon wave packet. We note that  $\hat{\epsilon}_{10}$  and  $\hat{\epsilon}_{20}$  are the positive frequency parts of the probe and FWM field operators at the entrance of the medium. Thus,  $\langle \hat{\epsilon}_{10}^\dagger \hat{\epsilon}_{10} \rangle$  and  $\langle \hat{\epsilon}_{20}^\dagger \hat{\epsilon}_{20} \rangle$  are proportional to the input single-photon probe field

intensity and the vanishing initial FWM field intensity at the entrance of the medium, respectively. In addition,

$$\begin{aligned}
 W_+ &= -\frac{2K_{12}^*\Omega_1\Omega_2d_1}{W}, \quad W_- = -\frac{2K_{12}\Omega_1^*\Omega_2^*d_3}{W}, \\
 \beta_{\pm} &= -\frac{i}{2} \left[ \frac{|\Omega_1|^2(K_2d_1 - K_1d_4) + K_2d_1d_2d_3}{D(0)d_1} \mp D_5(0) \right], \\
 \frac{1}{V_{g\pm}} &= \frac{1}{c} + \frac{1}{2d_1D(0)} \{ [K_1|\Omega_1|^2 + K_2(d_2 - d_3)d_1] \\
 &\quad \mp D_6(0) - [|\Omega_1|^2(K_2d_1 - K_1d_4) + K_2d_1d_2d_3 \\
 &\quad \mp D_7(0)] \frac{D_8(0)}{D(0)} \}, \tag{17}
 \end{aligned}$$

in which

$$\begin{aligned}
 W &= |\Omega_1|^2(K_1d_4 + K_2d_1) + K_2d_1d_2d_3 - D_7(0), \\
 D(0) &= d_2d_3d_4 + |\Omega_1|^2d_4 - |\Omega_2|^2d_3, \\
 D_5(0) &= D_7(0)/(d_1D(0)), \\
 D_6(0) &= \frac{-1}{D_7(0)} \{ [|\Omega_1|^2(K_1d_4 + K_2d_1) + K_2d_1d_2d_3] \\
 &\quad \times [K_1|\Omega_1|^2 + K_2(d_3 - d_2)d_1] + 2d_1|K_{12}\Omega_1\Omega_2|^2 \}, \\
 D_7(0) &= [ (|\Omega_1|^2(K_1d_4 + K_2d_1) + K_2d_1d_2d_3)^2 \\
 &\quad - 4|K_{12}\Omega_1\Omega_2|^2d_3d_1 ]^{1/2}, \\
 D_8(0) &= (d_2 - d_3)d_4 - d_2d_3 - |\Omega_1|^2 - |\Omega_2|^2. \tag{18}
 \end{aligned}$$

Equations (15) and (16) indicate that in general each frequency component of the probe and the generated FWM fields contains two propagation modes (wavepackets) that travel with different yet individually matched group velocities. In addition, both propagation modes (wavepackets) retain a pulse shape identical to that of the input probe field.

### B. Analysis of group velocities and propagation parameters

Before a detailed analysis we first consider a limiting case where  $\Omega_2 = 0$  and  $g_2 = 0$ . In this limit, our scheme reduces to that of a single  $\Lambda$  scheme. Using Eq.(9) we immediately obtain (note that when  $g_2 = 0$ ,  $D_2(\omega) = 0$ ), thus  $\hat{\epsilon}_1(z, \omega) = \hat{\epsilon}_{10}(0, \omega)e^{-i\lambda_0 z}$  where  $\lambda_0 = \omega/c + D_1(\omega)$ . This leads to a group velocity

$$V_{g_0} = \frac{c}{1 - \frac{cK_1|\Omega_1|^2}{d_1^2d_2^2}} \approx \frac{-d_1^2d_2^2}{K_1|\Omega_1|^2}, \left( \left| \frac{cK_1|\Omega_1|^2}{d_1^2d_2^2} \right| \gg 1 \right). \tag{19}$$

Alternatively, one can also obtain this result using Eq. (12). Note that with  $\Omega_2 = 0$  and  $g_2 = 0$ , we have  $D_2(\omega) = D_3(\omega) = D_4(\omega) = 0$ ,  $D_5(\omega) = D_1(\omega)$ ,  $U_+ = U_- = 0$ , and  $\lambda_- = \lambda_0 = \omega/c + D_1(\omega)$  and  $\hat{\epsilon}_1(z, \omega) = \hat{\epsilon}_{10}(0, \omega)e^{-i\lambda_0 z}$ . Equation (19) is the exact same superluminal group velocity obtained by Payne and Deng [7] in an atomic amplitude treatment of a single  $\Lambda$  active Raman gain scheme.

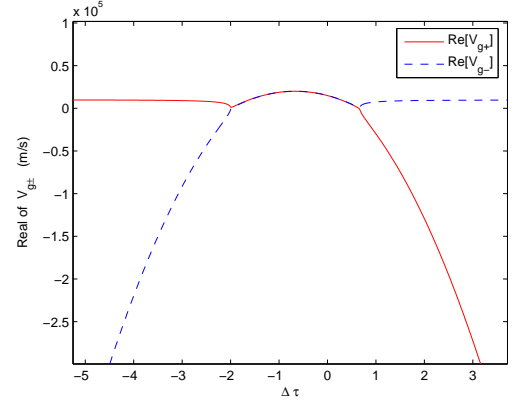


FIG. 2: (Color online) Group velocities  $V_{g\pm}$  as function of dimensionless two-photon detuning  $\Delta\tau$  for  $K_1 = K_2 = K_{12} = 1 \times 10^8/(\text{cm}\cdot\text{s})$ ,  $|\Omega_1| = 10$  MHz,  $|\Omega_2| = 10$  MHz,  $\tau = 10$   $\mu\text{s}$ ,  $\delta_1 = 1.5$  GHz,  $\delta_4 = 1$  MHz,  $\gamma_{31} = 300$  Hz,  $\gamma_{21} = \gamma_{23} = 5$  MHz, and  $\gamma_{41} = \gamma_{43} = 5$  MHz.

In general, for an injection-seeded double- $\Lambda$  active gain system each field consists, as indicated in Eqs. (12) and (13), of two propagation modes characterized by the eigenvalues  $\lambda_{\pm}$ , and therefore different group velocities  $V_{g\pm}$  and decay rates. For a short propagation distance where the decay of individual mode is not significant, these modes will overlap each other. For a sufficiently long propagation distance, however, modes with different propagation velocities will separate and the fast decay components decay out completely. Consequently, one obtains a pair of well-matched waves traveling with the identical group velocity and have the identical decay behavior.

In Fig. 2 we plot group velocities of each propagation mode (wavepacket) as a function of dimensionless two-photon detuning  $\Delta\tau$  for a typical cold alkali vapor where states  $|2\rangle$  and  $|4\rangle$  belong to the same hyperfine manifold. When the two-photon detuning is large, i.e.,  $\Delta\tau > 1$ , one wavepacket mode travels with a negative (superluminal) group velocity and the other wavepacket mode travels with a positive (subluminal) group velocity that can be substantially smaller than the speed of light in vacuum. In this case, the fast and slow modes separate quickly even before the differential decays become significant. Consequently, one obtains two group velocity-matched probe-FWM field pairs arriving at the detector at a delayed time [13].

When the two-photon detuning is small both propagation modes travel with positive group velocities. Depending on the group velocity difference and differential decay rates, one may obtain only one pair of group-velocity matched fields for a sufficiently long medium so that one of the eigenvalue has decayed out completely.

The above described propagation characteristics can also be understood from Eqs. (15) and (16) where parameters  $\beta_{\pm}$  describe the propagation characteristics of probe and generated fields. The case of  $\text{Re}[\beta_{\pm}] > 0$

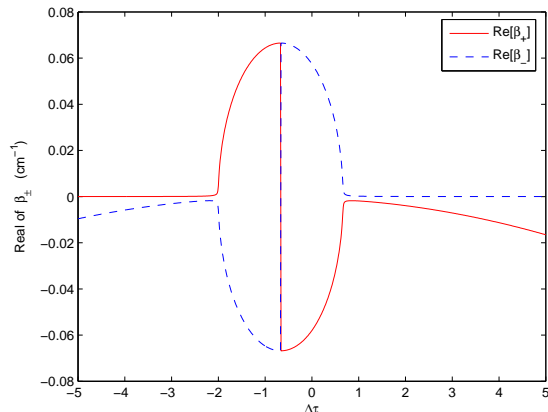


FIG. 3: (Color online) The coefficients  $\text{Re}[\beta_{\pm}]$  versus the dimensionless two-photon detuning  $\Delta\tau$ . The parameters are the same as Fig. 2.

corresponds to gain whereas  $\text{Re}[\beta_{\pm}] < 0$  indicates field attenuation. In Fig. 3 we show these propagation parameters as functions of the dimensionless two-photon detuning  $\Delta\tau$ . In the region where both propagation modes (wavepackets) travel with positive group velocities one propagation mode experiences amplification whereas other propagation mode is attenuated. Note also that near  $\Delta\tau \approx -0.665$  the signs of propagation constant change and the amplified (attenuated) mode becomes attenuated (amplified). These features are very different from the conventional EIT based FWM schemes where probe attenuation and FWM gain always occur. This is precisely due to the fact that EIT process is based on the weak absorption of the probe field and stimulated generation of the FWM field. In the case of active Raman gain medium, the probe field serves as an injection seeding source and it works in a stimulated emission mode. Consequently, simultaneous gain to both probe and FWM fields are possible. Indeed, if parameters are chosen such as  $\text{Re}[\beta_{+}] < 0$  and  $\text{Re}[\beta_{-}] > 0$ , then after a sufficient propagation distance, both the probe and FWM fields have the same gain feature characterized by  $\text{Re}[\beta_{-}] > 0$ . The energy that supports this bi-field increase comes from the two CW classical fields  $E_{P1}$  and  $E_{P2}$ .

### III. GENERATION OF GROUPED AND PAIRED PHOTONS

In this section, we consider the case where the input probe quantum state corresponds to a single-photon wave-packet state [14, 15]:

$$|1\rangle = \int_{-\infty}^{\infty} d\omega' \xi(\varpi + \omega') \hat{a}^{\dagger}(\omega') |0\rangle, \quad (20)$$

where the amplitudes  $\xi(\varpi + \omega')$  are normalized such that  $\int_{-\infty}^{\infty} d\omega' |\xi(\varpi + \omega')|^2 = 1$  and the  $\varpi$  is central frequency of wave packet. The initial state of the system is

$$|\psi(0)\rangle = |1\rangle_3 |0\rangle_4, \quad (21)$$

where subscripts 3 and 4 denote single photon wave packet of central frequency  $\omega_3$  and  $\omega_4$ , respectively. The state can be expanded in the boson Fock space as

$$|\psi(t)\rangle = \sum_{nm} \alpha_{nm}(z, t) |n\rangle_3 |m\rangle_4, \quad (22)$$

where  $n$  and  $m$  denote the photon numbers of central frequency  $\omega_3$  and  $\omega_4$ , respectively and  $\sum_{nm} \alpha_{nm}(z, t) = 1$ .

From the initial state Eq. (21) and by using the following relation

$$\begin{aligned} \langle i | F(\hat{E}_k^{(-)}, \hat{E}_l^{\dagger}, \hat{E}_k^{(-)}, \hat{E}_l^{(+)}, \dots) | i \rangle \\ = \langle f | F(\hat{a}_k^{\dagger}, \hat{a}_l, \hat{a}_k^{\dagger} \hat{a}_l, \dots) | f \rangle, \end{aligned} \quad (23)$$

where  $|i\rangle$  and  $|f\rangle$  are the initial and final states of the system, respectively, we can obtain the final state of the form Eq. (22).

#### A. Generation and analysis of (2+1) photon group

To generate a (2+1)-group of photons we consider the weak gain limit in which the injected single probe photon will stimulatedly generate only one photon in the probe frequency mode. Thus, only one atom is flipped from state  $|1\rangle$  to state  $|3\rangle$  via a two-photon Raman process. For this case we only consider:  $n, m \in \{0, 1, 2\}$ . Starting from Eq. (22) and taking the energy conservation into consideration, the state can be written as

$$|\psi(t)\rangle = \beta_{10} |1\rangle_3 |0\rangle_4 + \beta_{20} |2\rangle_3 |0\rangle_4 + \beta_{21} |2\rangle_3 |1\rangle_4. \quad (24)$$

Here, the physical meaning of each term is very clear.  $\beta_{10}$  represents the probability amplitude of the injected single probe photon not initiating a stimulated emission.  $\beta_{20}$  described the occurrence of the stimulated emission but no FWM generation. With suitable second pump field this amplitude can be made very small, indicating the high probability of generating a FWM photon, which is described by the probability amplitude  $\beta_{21}$ . Indeed, because photon creation and annihilation in pairs  $\{\hat{a}_1 \hat{a}_1, \hat{a}_1 \hat{a}_2, \dots, \hat{a}_2^{\dagger} \hat{a}_2^{\dagger}, \hat{a}_1 \hat{a}_1 \hat{a}_1 \hat{a}_2^{\dagger}, \dots, \hat{a}_2^{\dagger} \hat{a}_2^{\dagger} \hat{a}_2^{\dagger} \hat{a}_2^{\dagger}\}$  and because of the initial state Eq. (21), one can show that for our weak gain limit where only one photon in the probe frequency is stimulatedly generated the state vector can be expressed as

$$|\psi(t)\rangle = \beta_{10} |1\rangle_3 |0\rangle_4 + e^{-i\phi} \beta_{21} |2\rangle_3 |1\rangle_4, \quad (25)$$

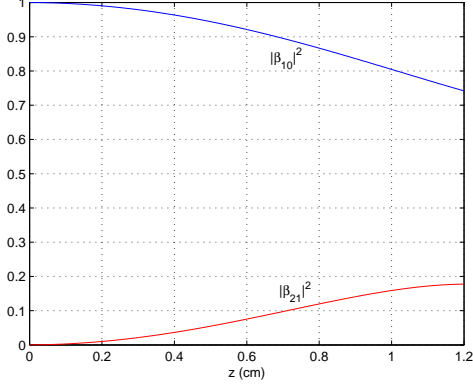


FIG. 4: (Color online) The probabilities  $|\beta_i|^2$  ( $i = 10, 21$ ) versus the  $z$  for  $|\Omega_1| = 10$  MHz,  $|\Omega_2| = 10$  MHz,  $\tau = 10$   $\mu$ s,  $K_1 = K_1 = K_{12} = 5 \times 10^8$ /(cm·s),  $\Delta\tau = -1$  MHz,  $\delta_1 = 1.5$  GHz,  $\delta_4 = 1$  MHz,  $\gamma_{31} = 300$  Hz,  $\gamma_{21} = \gamma_{23} = 5$  MHz, and  $\gamma_{41} = \gamma_{43} = 5$  MHz.

where

$$\begin{aligned} |\beta_{10}|^2 &= 1 - 2|A_2|^2|P_{p1}(\eta_+)e^{\beta_+z} - P_{p1}(\eta_-)e^{\beta_-z}|^2, \\ |\beta_{21}|^2 &= 2|A_2|^2|P_{p1}(\eta_+)e^{\beta_+z} - P_{p1}(\eta_-)e^{\beta_-z}|^2, \\ \phi &= -\arg[(W_+W_-P_{p1}(\eta_+)e^{\beta_+z} - P_{p1}(\eta_-)e^{\beta_-z}) \\ &\quad \times (P_{p1}(\eta_+)e^{\beta_+z} - P_{p1}(\eta_-)e^{\beta_-z})^*W_-^*]. \end{aligned} \quad (26)$$

In Fig. 4 we plot the two probabilities described in Eq. (25) for the propagation length of  $z=1$  cm. We note that for higher concentration and longer propagation distance, more than one probe photon can be generated and Eq. (25) will contain terms such as  $|3\rangle_3|2\rangle_4$ , etc.

The second term in Eq. (25) is very useful in various photon pair-based experiments. This term represents the situation of simultaneous existence of two photons in the probe frequency mode ( $\omega_3$ ) and one photon in the FWM frequency mode ( $\omega_4$ ). This is very different from the usual spontaneous down conversion schemes where two photons are produced simultaneously with one photon being in each frequency mode. Such a (1+1) generation significantly limits the subsequent experiments where the propagation of a paired photon are required since very often one of the photon is needed for coincidence counter purpose. With our scheme a 50-50 beam splitter (note it is simple to choose the wave vectors of the fields so that the probe and FWM photons can be directionally separated) can take one probe photon out for the coincidence triggering, leaving a fully correlated photon pair for the subsequent correlated pair propagation experiments. This opens a door for many paired-propagation related experimental studies.

In the subluminal propagation region  $|\Delta\tau| < 1$  (see Fig. 2), the final state of system is approximate as

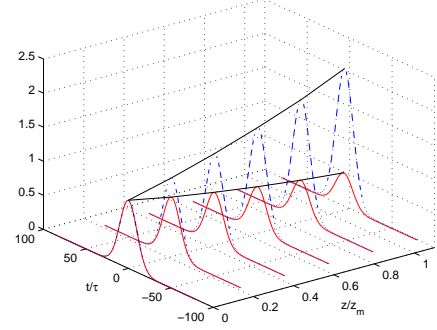


FIG. 5: (Color online) The wave packets of the  $V_{g+}$  mode (solid line) and  $V_{g-}$  mode (dashed-dot line) as function of the dimensionless  $z/z_m$  and  $t/\tau$ .  $K_{12} = K_1 = K_2 = 1 \times 10^9$ /(cm·s), and  $\Delta\tau = -0.2$ ,  $z_m = 1$  cm. The other parameters are the same as Fig. 2.

$$\begin{aligned} |\psi(t)\rangle &\approx P_{p1}(\eta_+)e^{\text{Re}[\beta_+]z}[\sqrt{|A_1|^2 - 3|A_2|^2}|1\rangle_3|0\rangle_4 \\ &\quad \pm e^{-i\phi}\sqrt{2}|A_2||2\rangle_3|1\rangle_4] \\ &\quad + P_{p1}(\eta_-)e^{\text{Re}[\beta_-]z}[\sqrt{|A_1|^2 - 3|A_2|^2}|1\rangle_3|0\rangle_4 \\ &\quad \mp e^{-i\phi}\sqrt{2}|A_2||2\rangle_3|1\rangle_4]. \end{aligned} \quad (27)$$

To better understand field propagation, the state (25) can be written as state (27) based on two different modes. The simulated propagation dynamics using a Gaussian wave packet is illustrated in Fig. 5. Note that each mode corresponds to a wave packet which consists of a superposition state composed of fields  $\hat{E}_1$  and  $\hat{E}_2$ . According to above-discussed  $V_{g\pm}$  and  $\text{Re}[\beta_{\pm}]$ , in the subluminal propagation region one mode gains and the other mode attenuates which is seen from Fig. 5.

## B. Glauber two-photon correlation function

We now discuss the important issue of Glauber two-photon correlation function of time delay  $\tau$  between the paired photons ( $\omega_3, \omega_4$ ). This correlation function can be expressed as

$$g_{E_1-E_2}^{(2)}(\tau) = \frac{\langle \hat{E}_1^{(-)}(t)\hat{E}_2^{(-)}(t+\tau)\hat{E}_2^{(+)}(t+\tau)\hat{E}_1^{(+)}(t) \rangle}{\langle \hat{E}_1^{(-)}(t)\hat{E}_1^{(+)}(t) \rangle \langle \hat{E}_2^{(-)}(t+\tau)\hat{E}_2^{(+)}(t+\tau) \rangle}. \quad (28)$$

The second-order normalized correlation function  $g_{E_1-E_2}^{(2)}(\tau)$  is illustrated in Fig. 6 and shows the anti-bunching nature, which implies a finite time delay for the emission of the second quantum field photon ( $\omega_4$ ). In other words, a nonclassical photon pair composed of frequencies  $\omega_3$  and  $\omega_4$  is generated in atomic vapors.

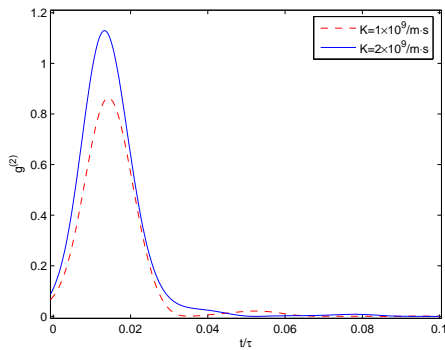


FIG. 6: (Color online) The second-order normalized correlation function versus dimensionless  $t/\tau$  for  $K_{12} = K_1 = K_2 = K$ ,  $|\Omega_1| = 10$  MHz,  $|\Omega_2| = 20$  MHz,  $\Delta\tau = -1$  and  $z = 0.8$  cm. The other parameters are the same as Fig. 2.

### C. Single-photon added coherent state

Here we consider injection of a weak coherent state  $|\alpha\rangle$  into the medium instead of a single probe photon  $|1\rangle$ . Using this system, we can prepare the single-photon-added coherent states (SPACs) [18, 19]. Photon-added coherent states  $(|\alpha, m\rangle = k_{\alpha, m} \hat{\epsilon}^{\dagger m} |\alpha\rangle)$ ,  $k_{\alpha, m}$  being a normalization constant and  $m$  an integer) [18] are the result of successive elementary one-photon excitations of a classical coherent field, and they occupy an intermediate position between the Fock and the coherent states, reducing to the two limit cases for  $\alpha \rightarrow 0$  or  $m \rightarrow 0$ . From Eq. (25), we know that the output mode will obtain the SPACS  $|\alpha, 1\rangle$  when the state  $|1\rangle_4$  is detected.

## IV. DISCUSSION

In deriving equations of motions for atomic dynamics we have neglected terms such as  $|\Omega_{1,2}|^2 / (\delta_4 - \delta_1 - i\gamma_{42})$ . In this section we first discuss these ac Stark-like frequency shifts. From Eq. (9) and Eq. (10), we obtain the phase mismatching induced by Stark shift

$$\Delta k_{\text{shift}} = \text{Re}[D_1(\omega) - D_4(\omega)]. \quad (29)$$

Figure 7 shows phase mismatching induced by the Stark shift versus  $\omega\tau$  by numerical calculations. It is clear from a comparison between Fig. 7 and Fig. 8 that the mismatching  $\Delta k_{\text{shift}}$  induced by Stark shift is very small with the exclusion of two maximal phase mismatches occur in the regions where the gain coefficients are maximized. From Fig. 7 we also obtain that the magnitude of two maximal phase mismatches are small compared with that of the wave vector of light field, so the angle of departure of field  $\vec{E}_2$  from the direction determine by  $\Delta \vec{k} \cdot \vec{r} \approx 0$  is small.

We also note that our scheme is of the deterministic nature. Once the probe light is introduced, we can deterministically (but time probabilistic-wise) obtain a group

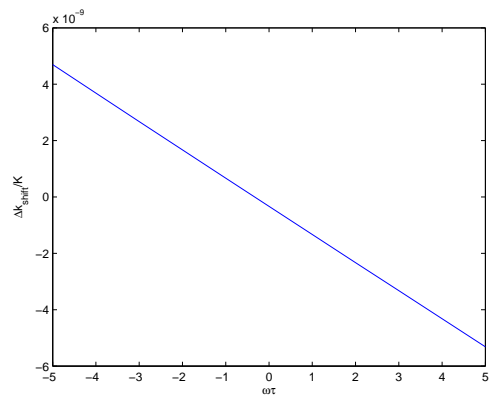


FIG. 7: (Color online) Phase mismatching induced by Stark shift  $\Delta k_{\text{shift}}$  as function of detuning  $\omega\tau$  for  $K = K_1 = K_2$  and  $\Delta\tau = -1$ . The other parameters are the same as Fig. 2.

of (2+1) photons at the same time. In order to obtain the desired result, the Raman gain (by the pump field Rabi frequency  $\Omega_1$ ) should be kept very low to ensure the stimulated generation of one probe photon. Of course, the pump field Rabi frequency  $\Omega_2$  should be kept appropriately to insure the unit conversion from state  $|3\rangle$  to state  $|4\rangle$  which leads to the simultaneous generation of one FWM photon.

We further note that with sufficient  $\Omega_2$  our scheme has approximately a EIT type behavior, as can be seen from the Hamiltonian (1). In this case, our four-level system is a hybrid system which is composed of an effective EIT (for the FWM photon generation) and Raman gain (for the probe photon generation). Specifically, consider the limiting case where  $\delta_4 = 0$ ,  $\Delta = 0$ ,  $|\Omega| = |\Omega_1| = |\Omega_2|$ , and very large one-photon detuning  $\delta_1$ , we find that the group velocity  $\frac{1}{v_g} = \frac{1}{v_{g+}} = \frac{1}{v_{g-}} \approx \frac{1}{c} + \frac{K}{2|\Omega|^2}$  which is EIT-like.

Next, we discuss the bandwidth of the Raman gain and the spatial width of single photons wave packet. From the Fig. 2 we know the magnitude of Raman gain bandwidth is ten MHz. The injecting seed single-photon wave-packet should be microsecond or sub-microsecond pulse. Figure 8 depicted the Raman gain in the Fourier transform space for the parameters used. As expected, the gain is small and rather flat as required.

Finally, we point out that the effect of quantum noises from the atomic system is ignored since the terms of Langevin-noise operators are excluded in Eq.(2). The ignorance of quantum noises is valid here as we exploit only the low-gain regime of the active-Raman gain medium for the purpose of generation of correlated photons.

## V. CONCLUSION

In conclusion, we have studied a (2+1)-photon generation scheme using a life-time broadened four-state atomic

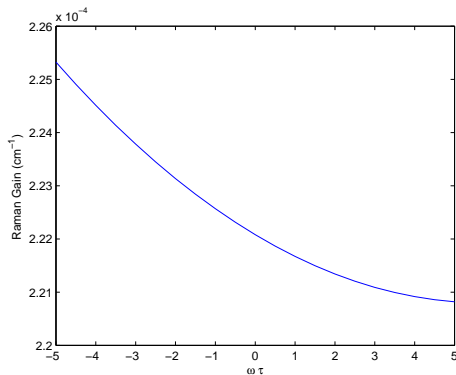


FIG. 8: (Color online) Frequency-dependent gain coefficient for the probe field as function of detuning  $\omega\tau$  for  $K_1 = 1 \times 10^8 / (\text{cm}\cdot\text{s})$ ,  $\Delta\tau = -1$ . The other parameters are the same as Fig. 2.

system. This scheme is based on a double- $\Lambda$  excitation configuration with the first  $\Lambda$ -branch forming an active-Raman-gain medium. This is very different from the conventional SPDC scheme. Furthermore, it is different from the spontaneous emission based biphoton generation scheme because the injection-seeding mechanism. This injection-seeding technique leads to the highly directional generation of desired photons, resulting in high detection efficiency. An important feature of the present scheme is that two identical probe photons, because of the stimulated Raman emission process due to injection-seeding, and a FWM photon are generated simultane-

ously, yielding a correlated and entangled (2+1) photons. Consequently, one of the probe photon can be used as a coincidence trigger whereas the remaining probe and FWM photons form a correlated and entangle pair that allows further experimental studies of paired propagation. We note that the conventional SPDC and the EIT schemes based on spontaneous Raman emission do not have such a capability. We finally note that with suitable driving conditions the injection-seeding scheme studied here can be generalized to produce groups of correlated and entangled photon groups for other type of experiments.

### Acknowledgments

This work was supported by the National Natural Science Foundation of China under Grants No.10588402 and No.10474055, the National Basic Research Program of China (973 Program) under Grant No. 2006CB921104, the Science and Technology Commission of Shanghai Municipality under Grants No. 06JC14026 and 05PJ14038, the Program for Changjiang Scholars and Innovative Research Team in University, Shanghai Leading Academic Discipline Project No. B408, the Research Fund for the Doctoral Program of Higher Education No. 20040003101. C.H. Yuan was supported by the China Postdoctoral Science Foundation (No. 20070410703) and Shanghai Postdoctoral Scientific Program.  
Email:†wpzhang@phy.ecnu.edu.cn

- 
- [1] A. Kuzmich, W. P. Bowen, A. D. Boozer, A. Boca, C. W. Chou, L.-M. Duan, and H. J. Kimble, *Nature* **423**, 731 (2003); S. V. Polyakov, C. W. Chou, D. Felinto, and H. J. Kimble, *Phys. Rev. Lett.* **93**, 263601 (2004).
- [2] C. H. van der Wal, M. D. Eisaman, A. André, R. L. Walsworth, D. F. Phillips, A. S. Zibrov, and M. D. Lukin, *Science* **301**, 196 (2003).
- [3] V. Balić, D. A. Braje, P. Kolchin, G.Y. Yin, and S. E. Harris, *Phys. Rev. Lett.* **94**, 183601 (2005).
- [4] P. Kolchin, S. Du, C. Belthangady, G. Y. Yin, and S. E. Harris, *Phys. Rev. Lett.* **97**, 113602 (2006).
- [5] J. K. Thompson, J. Simon, Huanqian Loh, V. Vuletić, *Science* **313**, 74 (2006).
- [6] Shengwang Du, Jianming Wen, Morton H. Rubin, and G.Y. Yin, *Phys. Rev. Lett.* **98**, 053601 (2007).
- [7] M. G. Payne and L. Deng, *Phys. Rev. A* **64**, 031802(R) (2001). Note for  $|\delta_1| \gg |\Delta|$  we have  $\delta_3 \approx \delta_1$ .
- [8] K. J. Jiang, L. Deng, and M. G. Payne, *Phys. Rev. A* **74**, 041803(R) (2006).
- [9] L. Deng and M. G. Payne, *Phys. Rev. Lett.* **98**, 253902 (2007).
- [10] L. J. Wang, A. Kuzmich, and A. Dogariu, *Nature (London)* **406**, 277 (2000).
- [11] It should be noted that the strong and far-detuned pump field  $E_{P1}$  can still generate a very weak spontaneous Raman emission at the frequency near the frequency of  $\omega_{23} - \delta_1$  when the probe field is absent (in the vacuum state) in the atomic medium. This process, however, can be distinguished and discriminated by the usual time-gating techniques. The Raman gain due to the first pump field should be small in order to generate only one photon in stimulated process.
- [12] L. Deng, M. G. Payne, G.X. Huang, and E.W. Hagley, *Phys. Rev. E* **72**, 055601(R) (2005).
- [13] L. Deng, M.G. Payne, and E.W. Hagley, *Phys. Rev. A* **70**, 063813 (2004).
- [14] U. M. Titulaer and R. J. Glauber, *Phys. Rev.* **145**, 1041 (1966).
- [15] M. G. Raymer, Jaewoo Noh, K.Banaszek, and I.A.Walmsley, *Phys. Rev. A* **72**, 023825 (2005).
- [16] V. Giovannetti, S. Lloyd, and L. Maccone, *Nature* **412**, 417 (2001).
- [17] O. Kuzucu, M. Fiorentino, M. A. Albota, F. N. C. Wong, and F. X. Käertner, *Phys. Rev. Lett.* **94**, 083601 (2005).
- [18] G. S. Agarwal, and K. Tara, *Phys. Rev. A* **43**, 492 (1991).
- [19] A. Zavatta, S. Viciani, and M. Bellini, *Science* **306**, 660 (2004).